Journal of Solid State Chemistry **143,** 224–229 (1999)
Article ID jssc.1998.8097, available online at http://www.idealibrary.com on IDEAL®

A New Nasicon-Type Phosphate $Co_{0.5}Ti_2(PO_4)_3$: I. Elaboration, Optical and Magnetic Properties

R. Olazcuaga,[1] J. M. Dance, and G. Le Flem

Institut de Chimie de la Matière Condensée de Bordeaux, CNRS - UPR 9048, 87, Avenue du Dr. A. Schweitzer, 33608 Pessac Cedex, France

J. Derouet, L. Beaury, and P. Porcher

Laboratoire de Chimie Métallurgique et Spectroscopie des Terres Rares, CNRS - UPR 209, 1, Place Aristide Briand, 92195 Meudon Cedex, France

and

A. El Bouari and A. El Jazouli

Laboratoire de Chimie des Matériaux Solides, Département de Chimie, Faculté des Sciences Ben M'Sik, Sidi Othmane, BP 6621, Casablanca, Morocco

Received February 28, 1997, in revised form November 4, 1998, accepted December 7, 1998

A new cobalt titanium monophosphate has been prepared by low temperature method. It crystallizes with the Nasicon-type structure. The indexation of the X-ray diffraction pattern is consistent with the $R\bar{3}$ or the $R32$ space groups. The atomic arrangement is a three-dimensional framework formed by PO_4 tetrahedra sharing corners with TiO_6 octahedra. Co^{2+} is located in half of the antiprism $M(1)$ sites in a centered ($R\bar{3}$) or off-centered ($R32$) position. The optical, EPR and magnetic data can account for a pure ionic Co–O bond. © 1999 Academic Press

I. INTRODUCTION

Nasicon-type phosphates have been extensively studied in the context of various fields of solid state chemistry: fast alkali–ion conductors (1), low thermal expansion ceramics (2), luminescence (3), and host structure for radioactive wastes (4). More recently, introduction of 3*d* ions as copper in this structure extends the potential application of such materials to various catalytic process, e.g., dehydrogenation and exchange reaction (5) and periodic catalytic activity (6). Within this scope a detailed investigation of the physical properties of the new Nasicon-type phosphate $Co_{0.5}Ti_2(PO_4)_3$ was undertaken.

This phosphate can be prepared without detectable impurities only by a low temperature method. The resulting low crystallinity makes such samples active in catalytic process but excludes an extended structural investigation. In this context, the object of this study—reported in two successive papers—will be to discuss the optical and magnetic properties in relation to a hypothetical cobalt environment. First, the crystallographic data will be discussed in relation to the crystal chemistry of the Nasicon-type phosphates. Then the optical absorption spectrum, the paramagnetic susceptibility, and the EPR parameters will be analyzed by the classical models deriving explicitly from the formalism of the Tanabe–Sugano diagrams and leading to a rough estimation of the crystal field parameter D_q and of the Racah parameter B.

In a second paper the physical properties will be simulated by using the Racah algebra calculation techniques. Such calculations have been carried out in the context of the simple overlap model developed by Malta (7) which have been successfully applied for reproducing the crystal field parameters of a great number of lanthanides as well as some 3*d* element compounds (8). This theoretical approach makes possible an exact determination of the cobalt–oxygen surroundings in so far as a slight change of the Co–O distance can be associated with a small variation of the crystal field parameters.

II. PREPARATION

The starting materials were diluted solutions of $Co(NO_3)_2$, $6H_2O$(I), $(NH_4)_2HPO_4$ (II) and $TiCl_4$ in ethanol (III). A slow addition of (III) in a (I) + (II) mixture at room temperature induces a precipitation. After drying at about 100°C the obtained amorphous violet powder is

[1]To whom correspondence should be addressed: ICMCB, Château Brivazac, 87, Avenue du Docteur A. Schweitzer, 33608 Pessac Cedex, France. Fax: 33(0) 5.56.84.27.61. E-mail: olaz@chimsol.icmcb.u-bordeaux.fr.

0022-4596/99 $30.00

progressively heated up to 750° C. The beginning of crystallization observed by X-ray diffraction (XRD) occurs at 660° C but the compound is stable only below 800° C. The lines of the XRD pattern remain broad even after a long annealing at 750° C which excludes a refinement of the crystal structure.

III. STRUCTURAL INVESTIGATION

The XRD pattern can be indexed assuming a rhombohedral cell (Table 1). The order of magnitude of the parameters in the equivalent hexagonal cell is typical of a Nasicon-type structure: $a = 8.510 \pm 0.003$ Å, $c = 21.04 \pm 0.005$ Å (Table 2). The densities ($d_{exp.} = 3.04\ g \cdot cm^{-3}$, $d_{calc.} = 2.94\ g \cdot cm^{-3}$) imply six $Co_{0.5}Ti_2(PO_4)_3$ formulae per unit-cell. The indexation of all reflections is consistent with the $R\bar{3}$ or $R32$ space groups (Table 1). According to these data the structure of $Co_{0.5}Ti_2(PO_4)_3$ consists of a tridimensional framework of PO_4 tetrahedra and TiO_6 octahedra sharing corners. The cobalt (II) ions are located in half of the usually labeled $M(1)$ sites, i.e., within the antiprism elongated along the c-axis and sharing faces with two TiO_6 octahedra. In the $R\bar{3}$ space group, Co^{2+} is found at the center of M(I) site (D_{3h} point symmetry) (Fig. 1) whereas in the context of the $R32$ space group, the cobalt atom can be displaced along the c axis giving rise to three short Co–O distances and to three longer distances (C_{3v} point symmetry) (Fig. 2). These results are consistent with the stability of the covalent $Ti_2(PO_4)_3$ skeleton which can accomodate ions of various sizes such as Li^+, Na^+, K^+, Mg^{2+}, Co^{2+}, Mn^{2+}, and Ca^{2+}. Actually the volume of the antiprism M(I) is related to the size of these cations but for the smallest ions this volume is obviously limited by the repulsive character of the oxygen nearest neighbors along the c axis. This limit corresponds to the minimum reached by the c/a ration 2.47 (Table 2).

Recently the structure of $Mn_{0.5}Ti_2(PO_4)_3$, which can be prepared at high temperatures, has been reported and solved in the $R\bar{3}$ space group ($a_h = 8.510 \pm 0.003$ Å; $c_h = 21.09 \pm 0.05$ Å) (9). The Mn–O distance in the M(1) site is 2.262 Å, i.e., close to the sum of the ionic radii (2.23 Å) (10). Assuming identical atomic coordinates for the cobalt phosphate, the calculated Co–O distance is 2.25 Å which is higher than the sum of the ionic radii (2.17 Å). Therefore the selection of the space group cannot be deduced only from these crystallographic data.

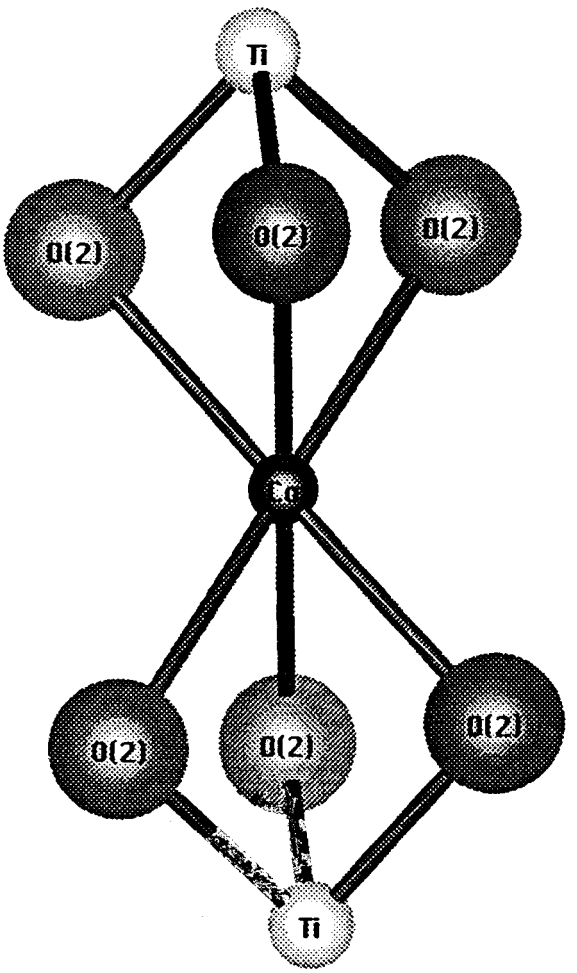

FIG. 1. Co^{2+} at the center of the M(1) site ($R\bar{3}$).

TABLE 1
Indexation of the X-Ray Powder Pattern of the As-Prepared $Co_{0.5}Ti_2(PO_4)_3$

hkl	$d_{obs.}$ (Å)	$d_{calc.}$ (Å)	I/I_0
(003)	7,18	(7,01)[a]	3
012	6,03	6,03	8
110	4,256	4,255	54
113	3,631	3,638	100
202	3,471	3,478	6
024	3,012	3,018	20
211	2,760	2,761	15
116	2,701	2,706	27
300	2,453	2,457	15
208	2,140	2,140	3
119		2,048	
	2,043		5
217		2,043	
128	1,912	1,912	13
0111	1,850	1,851	4
226		1,818	
	1,816		10
042		1,815	

[a] The rather broad line observed at this angle is possibly the signature of a stacking defect along the c axis.

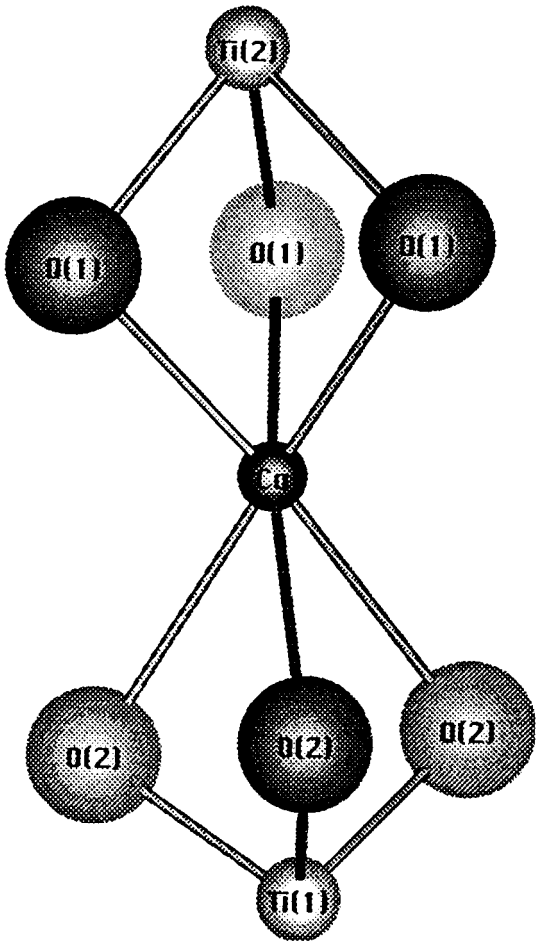

FIG. 2. Co^{2+} in off-centered position in the M(1) site (*R*32).

IV. OPTICAL PROPERTIES

The absorption spectrum was recorded using a double monochromator Cary 2400 spectrometer at 300 K and 12 K (Fig. 3). The spectrum can be divided into three regions labeled I, II, and III as the energy decreases.

In Region I the beginning of the charge transfer is observed at $\lambda = 350$ nm (3.56 eV); this value can be compared to those of TiO_2(11), $SrTiO_3$(11), and titanium phosphates of Nasicon-type structure (12–16) listed in Table 3. The origin of this absorption can be understood in terms of transition between orbitals mostly localized on oxygens and antibonding orbitals mostly localized on titanium. In $SrTiO_3$ the Ti–O bonds are more covalent than in TiO_2 due to the better overlap between 3*d* titanium and 2*p* oxygen orbitals in addition to the reinforcement of the Ti–O bond by the competing Sr–O bond. In the case of the phosphates, the rigid phosphotitanium framework involves a strong Ti–O bond and accordingly high *E* values.

The other regions correspond to the crystal field transition of Co^{2+}: Region II exhibits an intense and broad band partially resolved in the visible range (400–800 nm) and Region III exhibits less intense wider bands in the infrared domains (800–2000 nm). The ground state of the free Co^{2+} ($3d^7$) ion is ^4F. In an octahedral crystal field, the ^4F state splits into two orbital triplets $^4T_{1g}$ (ground level), $^4T_{2g}$, and one orbital singlet $^4A_{2g}$.

This absorption spectrum is due to the transitions between the ground level and the excited states (^4P, ^2G, ^2H,

TABLE 2
Cell Parameters of $M_xTi_2(PO_4)_3$ Phases (M = Li, Na, Mg, Co, Ca; x = 0.5 or 1)

Compounds	*a*(Å)	*c*(Å)	*c*/*a*	RM^+, M^{2+}(10)	Ref.
$LiTi_2(PO_4)_3$	8.518	20.87	2.45	0.76	12
$NaTi_2(PO_4)_3$	8.488	21.80	2.57	1.02	13
$KTi_2(PO_4)_3$	8.354	23.12	2.77	1.38	14
$Mn_{0.5}Ti_2(PO_4)_3$	8.520	21.09	2.48	0.83	9
$Mg_{0.5}Ti_2(PO_4)_3$	8.490	20.98	2.47	0.72	15
$Co_{0.5}Ti_2(PO_4)_3$	8.510	21.035	2.47	0.75	this work
$Ca_{0.5}Ti_2(PO_4)_3$	8.360	22.01	2.63	1.00	14

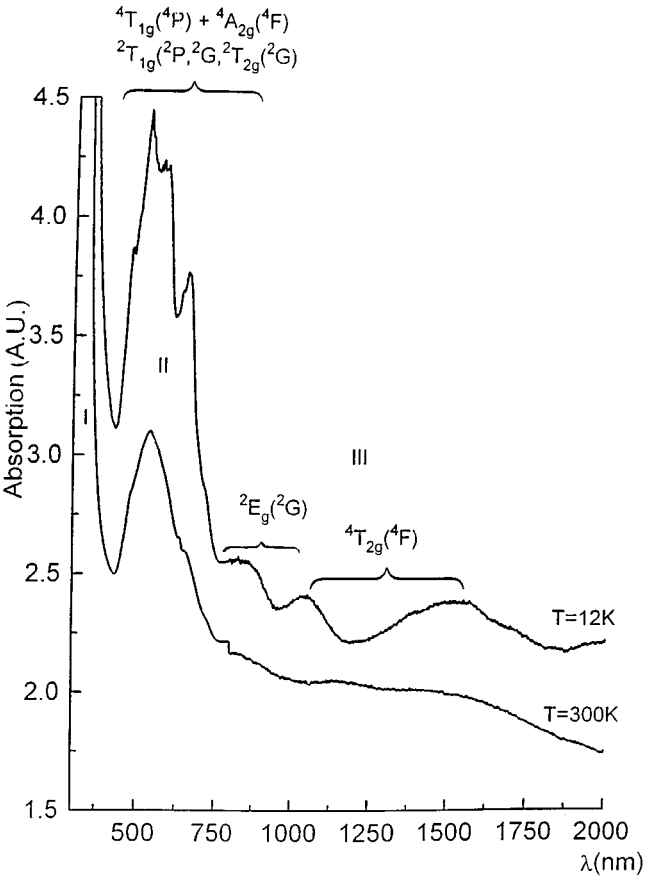

FIG. 3. Crystal field spectrum of $Co_{0.5}Ti_2(PO_4)_3$.

TABLE 3
Location of the Charge Transfer Band Found in Several Ti(IV) Oxides

Compounds	E (ev)	Ref.
TiO_2 (rutile)	3.00	11
$SrTiO_3$	3.40	11
$KTiOPO_4$	3.54	17
$NaTi_2(PO_4)_3$	3.54	13
$Na_5Ti(PO_4)_3$	3.50	18

^2D, ^2P, ...). The best resolution at 12 K and an attempt of deconvolution allow the establishment of the sequence of energy levels given in Table 4. From this table the mean positions of the spin allowed transitions $^4T_{1g}(^4F) \rightarrow {}^4T_{2g}(^4F)$, $^4A_{2g}(4F)$, $^4T_{1g}(^4P)$ were estimated approximately at 7530, 15220, and 19110 cm^{-1}. In a simple model ignoring the effects of the spin-orbit coupling and of the distortion of the cobalt site (19), these values permit the calculation of the ligand field parameter and the Racah parameter B: $D_q = 815\ cm^{-1}$, $B = 833\ cm^{-1}$.

Table 5 compares these values with those deduced from the optical spectra of various fluorides or oxides. Clearly this method gives a good estimation of D_q which is higher for oxides than for fluorides. The calculated value for $Co_{0.5}Ti_2(PO_4)_3$ is more significant of lower crystal fields than those usually found in oxides. The calculated Racah parameter B is typical of Co(II) oxides but cannot reflect accurately the nature of the Co–O bond.

V. EPR INVESTIGATION

The EPR spectrum of a polycrystalline sample of $Mg_{0.49}Co_{0.01}Ti_2(PO_4)_3$ has been recorded at 4.1 K, using a BRUKER ER 200tt X band spectrometer with a 100 KHz modulation. The dilution of cobalt in the isostructural magnesium phase gives a better resolution. The experimental values are $g_{\parallel} = 7.34$ and $g_{\perp} = 2.11$.

The ground level $^4T_{1g}$ splits into six Kramers doublets. This degeneracy is lifted in presence of an external magnetic field. The energies and g values can be calculated as a function of the spin–orbit coupling constant ξ, of the axial distortion δ of the octahedral site, and of the applied magnetic field $\mathbf{H}$ by using the hamiltonian (23,24)

$$\mathscr{H} = -1/3\gamma\xi\mathbf{L}\cdot\mathbf{S} - \delta(L_Z^2 - 2/3) + \beta\mathbf{H}(\gamma\mathbf{L} + g_e\mathbf{S}),$$

where γ satisfies $-3/2 \leq \gamma \leq -1$ ($-3/2$ in a weak field and -1 in a strong field). In the case of a ligand (p)–metal (d) mixing that can be considered as an indication of the cobalt–oxygen bond covalency we replace, in $\mathscr{H}$, $\mathbf{L}$ by $k\mathbf{L}$ ($k < 1$) and 2/3 by $2/3\,k^2$.

The g factors are calculated from the matrix elements

$$\langle \Psi_{\pm} | \gamma\mathbf{L} + g_e\mathbf{S} | \Psi_{\pm} \rangle,$$

$\Psi_{\pm}$ being the wave functions of the hamiltonian $\mathscr{H}$.

For a given γ, the two g values ($g_{\parallel}$ and $g_{\perp}$) are functions of a single parameter δ/ξ. Figure 4 gives $g_{\perp}$ versus $g_{\parallel}$ for $\gamma = -1$ and $-3/2$. For the limit cases $\delta = \pm\infty$ the g values are, respectively,

$$\delta = +\infty,\ g_{\parallel} = 2(3-\gamma),\ g_{\perp} = 0$$

$$\delta = -\infty,\ g_{\parallel} = 2,\ g_{\perp} = 4.$$

Obviously as $\delta = 0$ (cubic case), $g_{//} = g_{\perp} = 13/3$.

By introducing these data in the diagram of Fig. 4 a slight discrepancy is observed with theoretical calculation involving a low crystal field. The value of δ/ζ can be calculated assuming a pure ionic Co–O bond ($k = 1$). The best agreement is obtained for $\delta = 1170\ cm^{-1}$, $g_{\parallel} = 7.53$, and $g_{\perp} = 2.28$. These new data are consistent with the weak field prediction.

TABLE 4
Experimental Energy Levels Determined by Deconvolution of the Absorption Bands at 12 K

Infrared region		Absorption transition	Visible region		Absorption transition
λ (nm)	ν (cm^{-1})		λ (nm)	ν (cm^{-1})	
1691	5914		712	14045	
1560	6410		657	15220	$^4T_{1g}(^4F)$
1490	6711	$^4T_{1g}(^4F)$	594	16835	$\rightarrow {}^4T_{1g}(^4P)$
1377	7262	$\rightarrow {}^4T_{1g}(^4F)$	574	17422	$+ {}^4A_{2g}(^4F)$
1087	9200	$+ {}^2E_g(^2G)$	533	18762	$+ {}^2T_{1g}(^2P^2G)$
1033	9681		509	19646	$+ 2T_{2g}(^2G)$
845	11834		485	20619	
830	12048				

TABLE 5
Ligand Field Parameters Deduced from the Absorption Spectra of Octahedral Co(II) Compounds

Compounds	D_q(cm^{-1})	B (cm^{-1})	Ref.
$KMgF_3$: Co	800	880	20
$KCoF_3$	770	880	20
MgO : Co	960	833	21
$Na_4Co(P_3O_9)_2,6H_2O$	950	850	22
$(NH_4)_4Co(P_3O_9)_2,4H_2O$	950	833	22
$CoCl_2$	690	780	20
$CoBr_2$	640	760	20

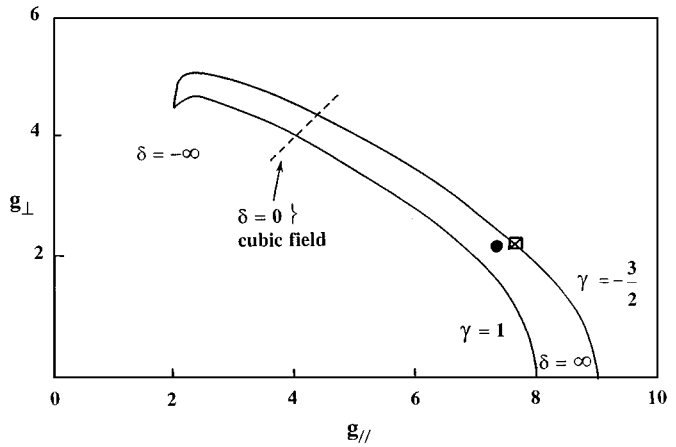

FIG. 4. Parametric variation of $g_\perp$ vs $g_\parallel$ for Co^{2+} ion according (24). The experimental points correspond to the data of $Co_{0.5}Ti_2(PO_4)_3$.

VI. MAGNETIC INVESTIGATION

The magnetic susceptibility of $Co_{0.5}Ti_2(PO_4)_3$ was recorded between 4.2 and 280 K using a Faraday balance. The $\chi^{-1} = f(T)$ curve is linear at high temperature and deviates slightly from the linearity at low temperature. The experimental Curie constant 3.16 is close to the value calculated assuming an orbital contribution ($C = 3.38$) . Such a curve is typical of a paramagnetic behavior of an isolated Co^{2+} ion located in a distorted octahedral site. The magnetic properties of a $^4T_1$ term in an axially symmetric crystal field have been described previously by Figgis *et al.* (25) who considered a simultaneous perturbation by the spin–orbit coupling λ and the axial crystal field variable δ. The terminal variation of the magnetic moment $\mu_{\text{eff.}}$ is expressed in terms of δ, k, and γ. Assuming $k = 1$ and $\gamma = -1.5$ the δ value giving the best fit to the experimental magnetic moment is 900 cm^{-1}, a value in good agreement with the distortion parameter inferred from EPR (Fig. 5).

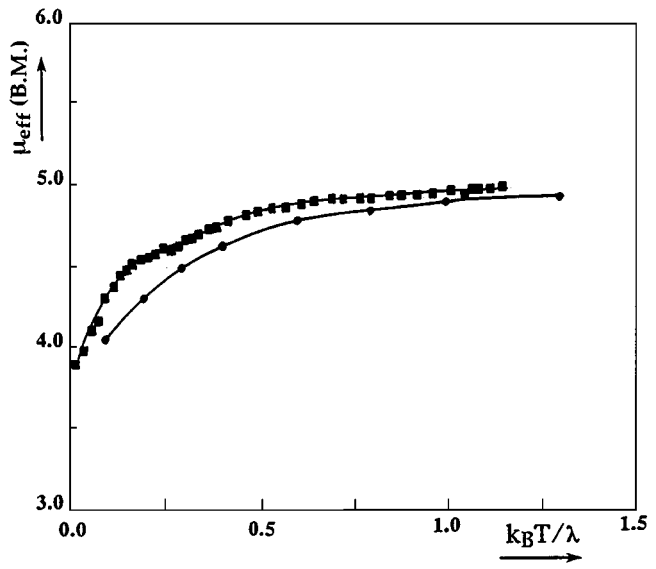

FIG. 5. Comparison between the experimental (■) and calculated (●) variation of μ_{eff} for $Co_{0.5}Ti_2(PO_4)_3$ (k_B is the Boltzmann's constant, $\lambda = -\xi/3$).

VII. CONCLUSIONS

$Co_{0.5}Ti_2(PO_4)_3$ belongs to the Nasicon-type family. The cobalt ions are located in half of the antiprismatic $M(1)$ sites in a centered or off-centered position. The value of the crystal field intensity deduced from the absorption spectrum $D_q = 815$ cm^{-1} is rather low for an oxide and evidences an ionic character of the Co – O bond. The deviation from the cubic symmetry of the cobalt site is consistent with the EPR and magnetic data: in this phosphate Co^{2+} has a high spin electronic configuration and the g values can be interpreted in the context of the weak field limit. Finally, as it was demonstrated in a previous study describing a family of cobalt cyclophosphates (22), Co^{2+} behaves as a probe extremely sensitive to its close environment and a clear analysis of the spectroscopic properties needs a precise determination of the crystal field parameters, which is the object of the forthcoming paper.

REFERENCES

1. J. B. Goodenough, H. Y. P. Hong, and J. Kafalas, *Mat. Res. Bull.* **11,** 203 (1976).
2. J. Alamo and R. Roy, *J. Amer. Ceram. Soc. C* **78,** No. 5 (1984).
3. P. Boutinaud, C. Parent, G. Le Flem, C. Pedrini, and B. Moine, *J. Phys.: Condens. Mater*, **4,** 3031 (1992).
4. R. Roy, D. K. Agrawal, J. Alamo, and R. A. Roy, *Mat. Res. Bull.* **19,** No. 2, 471 (1979).
5. L. Monceaux and P. Courtine, *Eur. J. Solid State Inorg.* Chem. **28,** 233 (1991).
6. A. Serghini, M. Kacimi, M. Ziyad, and R. Brochu, *J. Chim. Phys. (Paris)* **85,** No. 4, 499 (1988).
7. O. L. Malta, *Chem. Phys. Lett.* **88,** No. 4, 353 (1982).
8. P. Porcher, M. Couto Dos Santos, and O. Malta, *Phys. Chem. Chem. Phys.* **1** (1999), in press.
9. H. Fakrane, A. Aatiq, M. Lamire, A. El Jazouli, and C. Delmas, *Ann. Chim. Sci. Mater.* **23,** 81 (1998).
10. R. D. Shannon, *Acta Crystallogr. A* **32**, 75 (1976).
11. D. E. Scaife, *Sol. Energ.* **25,** 41 (1980).
12. R. Masse, *Bull. Soc. Fr. Minéral. Cristallogr.* **93,** 500 (1970).
13. L. Hagman and P. Kierkegaard, *Acta Chem. Scand.* **22,** 1822 (1968).
14. R. Masse, *Bull. Soc. Fr. Minéral. Cristallogr.* **95**, 47 (1972).
15. S. Barth, R. Olazcuaga, P. Gravereau, G. Le Flem, and P. Hagenmuller, *Mater Lett.* **16,** 96 (1993).
16. I. Makoto, K. Seichi, K. Akira, and K. Makio, *Nippon Kagaku* **11,** 1752 (1982).
17. J. D. Berlin and H. Vanderzeele, *J. Opt. Soc. Amer. B* **6,** 622 (1989).
18. S. Krimi, A. El Jazouli, L. Rabardel, M. Couzi, I. Mansouri, and G. Le Flem, *J. Solid State Chem.* **102,** 400 (1993).

19. E. Köning, "Structure and Bonding," Vol. 9, p. 175, Springer-Verlag, Berlin/New York, 1971.
20. J. Ferguson, K. Knok, and D. L. Wood, *J. Chem. Phys.* **39,** 881 (1963).
21. W. Low, *Phys. Rev.* **109,** No. 2, 256 (1958).
22. P. Caro, J. Derouet, M. Belkhiria, M. Ben Amara, M. Dabbabi, J. M. Dance, and G. Le Flem, *J. Chimie Phys.* (*Paris*) **91,** 293 (1994).
23. J. S. Griffith, "The Theory of Transition-Metal Ions," Cambridge Univ. Press, Cambridge, UK, 1964.
24. A. Abragam and M. H. L. Pryce, *Proc. Royal Soc.* (*London*), *A* **206,** 173 (1951).
25. B. N. Figgis, M. Gerloch, J. Lewis, F. E. Mabbs, and G. A. Webb, *J. Chem. Soc.* (*A*) 2086 (1968).